International Journal of Engineering and Technical Research (IJETR)
ISSN: 2321-0869 (O) 2454-4698 (P), Volume-15, Issue-1, June - December 2025

Coupled Electro-Thermal Analysis of Resistive SFCL for Fault Mitigation and Voltage Stability in High-Voltage Networks

Majed Mohammed Alzouri and Mohammed Gronfula

***Abstract*—This paper investigates the effectiveness of a resistive-type Superconducting Fault Current Limiter (SFCL) in mitigating short-circuit currents within a 230 kV multi-bus power system. A detailed coupled electro-thermal simulation model was developed in MATLAB/Simulink to analyze system behavior under severe three-phase-to-ground faults ($R_f = 0.05\ \Omega$). Unlike previous studies relying on simplified models, this work utilizes correct sub-transient generator modeling to produce realistic fault levels. Results demonstrate that the optimized SFCL reduces the peak fault current by 57.1% (from 11.2 kA to 4.8 kA) while significantly enhancing transient stability. Furthermore, the SFCL prevents voltage collapse, maintaining bus voltage at 72% of nominal (166 kV) compared to near-zero without protection, ensuring compliance with strict grid code ride-through requirements. The device exhibits a stable phase-plane trajectory with no thermal runaway, reaching a peak temperature of 180 K and reducing thermal stress (I^2t) on network components by over 80%. These findings validate the SFCL parameters as a robust solution for modern power grid resilience.**

***Index Terms*—Superconducting fault current limiter (SFCL), short-circuit current, transient analysis, multi-bus power system, MATLAB/Simulink, power system protection, high temperature superconductor (HTS), fault current mitigation.**

I. Introduction

A. Background and Motivation

The global expansion of power transmission networks and interconnected generation has enhanced reliability but critically increased short-circuit current levels [1]. These currents can reach dangerous magnitudes within milliseconds, offering significant safety and economic challenges by potentially damaging transformers and transmission infrastructure [2], [3].

B. Fault Current Problem Statement

Fault transients contain decaying DC offsets where the initial peak determines the mechanical and thermal stress on equipment [4]. In many modern networks, these currents exceed the interrupting ratings of existing circuit breakers. Facing the costly option of upgrading switchgear or the operational constraints of network modification [5], utilities urgently require cost-effective fault limiting solutions.

Majed Mohammed Alzouri is with the College of Engineering, Alasala Colleges, Dammam 31435, Eastern Province, Saudi Arabia (e-mail: 11800001@alasala.edu.sa).
Mohammed Gronfula is with the College of Engineering, Alasala Colleges, Dammam 31435, Eastern Province, Saudi Arabia (e-mail: mohammed.gronfula@alasala.edu.sa).
Corresponding author: Majed Mohammed Alzouri.

C. Traditional Protection Methods and Limitations

Conventional mitigation includes upgrading breakers, series reactors, or network splitting. However, upgrading is capital-intensive; series reactors introduce constant voltage drops and power losses [6]; and network splitting compromises reliability and flexibility [7]. These limitations necessitate advanced active solutions like Superconducting Fault Current Limiters (SFCLs).

D. Introduction to SFCL Technology

SFCLs utilize the quenching property of superconductors to provide a distinct protection approach. They exhibit negligible impedance during normal operation but rapidly transition to a high-resistance state upon fault inception, limiting current within milliseconds [8], [9]. Unlike fuses, SFCLs automatically recover after fault clearance [3]. Among the various topologies, resistive-type SFCLs using High-Temperature Superconductors (HTS) like YBCO are favored for their simplicity and effectiveness [10], [11].

E. Research Objectives and Scope

This research aims to quantify the effectiveness of resistive-type SFCLs in a realistic multi-bus power system. The specific objectives are:

1) Develop a detailed MATLAB/Simulink model of a multi-bus AC system for transient analysis.
2) Design a resistive-type SFCL model with realistic electrical and thermal dynamics.
3) Simulate severe three-phase faults to evaluate SFCL performance in limiting current and enhancing voltage stability.
4) Conduct parametric studies to optimize SFCL design parameters.

The scope focuses on balanced three-phase faults using coupled electro-thermal simulation, building upon prior work [12], [13] to provide practical design guidelines.

II. Literature Review

A. Evolution of Fault Current Limitation Technologies

Traditional protection using circuit breakers and fuses is increasingly insufficient for modern grids with rising fault levels. Zadeh et al. [6] noted the limitations of medium voltage breakers, suggesting metal oxide arresters as alternatives. However, the constraints of conventional methods in complex networks have accelerated the adoption of advanced solutions like SFCLs.

B. SFCL Classification and Types

SFCLs are primarily resistive, inductive, or hybrid. **Resistive SFCLs** are favored for their simplicity and ability to damp power oscillations [3], though thermal recovery remains critical [2]. **Inductive SFCLs** offer robustness via magnetic saturation [4] but are bulkier. **Hybrid SFCLs** combine these benefits; Shawel and Bekele [8] minimized material costs with a YBCO-based hybrid design, while Zhu et al. [9], [10] demonstrated that bias magnetic fields enable flexible control and reduced losses.

C. SFCL Modeling and Simulation Approaches

Accurate transient analysis requires robust modeling tools. MATLAB/Simulink is widely employed to simulate superconductor non-linearities [4], [10]. Advanced models integrate thermal dynamics, as Xie et al. [14] showed that coupling the temperature rise with electrical behavior is vital for ensuring device safety and thermal stability during faults.

D. SFCL Placement and Optimization

Optimal allocation balances performance and cost. Jo and Joo [12] utilized a "Minimax Regret Criterion" to minimize risk across fault scenarios. Economic feasibility is also paramount; Lee and Joo [5] argued that SFCL costs are offset by savings from deferred breaker upgrades. Furthermore, Lim and Kim [13] highlighted that SFCLs preserve relay coordination in systems with distributed generation.

E. SFCL Impact on System Stability

SFCLs significantly enhance stability. Wang et al. [7] found they prevent wind turbine disconnection during faults. In DC systems, Yehia and Taha [1] applied SFCLs as "virtual inertia" to suppress voltage oscillations, while Ma et al. [15] emphasized their role in maintaining synchronism for virtual synchronous generators.

F. Practical Implementations and Case Studies

Applications in critical infrastructure demonstrate SFCL value. Letèf et al. [16] showed their necessity for securing unmanned offshore platforms fed by long cables. On the component side, Zhu et al. [11] designed non-inductive units to minimize grid impact during normal operation.

G. Research Gap and Motivation

While extensive literature exists, most studies utilize simplified static models. The specific interplay between coupled electro-thermal SFCL dynamics and voltage stability in multi-source high-voltage meshes remains under-explored. This paper addresses this gap by developing a detailed coupled simulation to explicitly quantify the impact of dynamic thermal evolution on system voltage recovery.

III. Theoretical Background

This section outlines the fundamental principles of superconductivity, the operating mechanism of the Superconducting Fault Current Limiter (SFCL), and the mathematical basis for short-circuit current analysis.

A. Fundamentals of Superconductivity

Superconductivity is a phenomenon where certain materials exhibit zero electrical resistance and the expulsion of magnetic flux fields when cooled below a characteristic critical temperature (T_c). For power system applications, High-Temperature Superconductors (HTS), such as Yttrium Barium Copper Oxide (YBCO), are preferred because they can operate at liquid nitrogen temperatures (77 K), which is more practical and economical than liquid helium cooling [8].

The state of a superconductor is defined by three critical parameters:

- Critical Temperature (T_c)
- Critical Current Density (J_c)
- Critical Magnetic Field (H_c)

If any of these parameters exceeds its critical limit, the material transitions from the superconducting state (zero resistance) to the normal state (high resistance). This transition, known as "quenching," is the core principle behind the operation of resistive SFCLs [10].

B. SFCL Operating Mechanism

The resistive-type SFCL functions as a variable resistor dependent on current density (J) and temperature (T). During normal operation ($I < I_c$), it offers negligible impedance. Upon a fault ($I > I_c$), the device quenches, transitioning to a high-resistance state within milliseconds to limit the surge. The resistivity $\rho(t)$ follows a power-law relationship [4]:

$$\rho(t) = \begin{cases} 0 & \text{if } J < J_c \text{ (Superconducting)} \\ \rho_n \left(\frac{J}{J_c}\right)^n & \text{if } J \geq J_c \text{ (Quenching)} \\ \rho_n & \text{if } T > T_c \text{ (Normal State)} \end{cases} \quad (1)$$

Where:

- ρ_n is the normal state resistivity.
- n is the flux creep exponent (typically $n > 20$ for YBCO).
- J is the instantaneous current density.
- J_c is the critical current density.

The thermal behavior of the SFCL during a fault is governed by the heat balance equation [14]:

$$Q_{sc}(t) = \int I(t)^2 R_{sc}(t)\, dt \quad (2)$$

$$T(t) = T_0 + \frac{1}{C_{sc}} \int (P_{gen}(t) - P_{cool}(t))\, dt \quad (3)$$

Where Q_{sc} is the generated heat, T_0 is the initial temperature, C_{sc} is the heat capacity, P_{gen} is the generated power (I^2R), and P_{cool} is the cooling power dissipated to the liquid nitrogen bath.

C. Short-Circuit Current Analysis

A short-circuit fault in a power system results in a transient current surge. For a symmetrical three-phase fault, the fault current $i_f(t)$ consists of a steady-state AC component and a decaying DC component [3]:

$$i_f(t) = \frac{V_{max}}{Z}\left[\sin(\omega t + \alpha - \phi) - e^{-t/\tau}\sin(\alpha - \phi)\right] \quad (4)$$

Where:

- V_{max} is the peak system voltage.
- $Z = \sqrt{R^2 + (\omega L)^2}$ is the system impedance.
- $\phi = \tan^{-1}(\omega L/R)$ is the impedance angle.
- α is the fault inception angle.
- $\tau = L/R$ is the time constant of the DC decay.

When an SFCL is inserted, the total impedance Z increases significantly during the fault, reducing the magnitude of the first term (AC component) and accelerating the decay of the second term (DC component) by decreasing the time constant τ [2].

The effectiveness of the SFCL is quantified by the current limiting ratio (CLR), defined as:

$$CLR(\%) = \frac{I_{no} - I_{SFCL}}{I_{no}} \times 100 \quad (5)$$

Where I_{no} and I_{SFCL} are the peak fault currents without and with the SFCL, respectively.

IV. System Modeling and Methodology

This section details the power system configuration and the SFCL mathematical modeling implemented in MATLAB/Simulink. The approach, summarized in Fig. 1, integrates coupled electro-thermal physics for rigorous transient analysis.

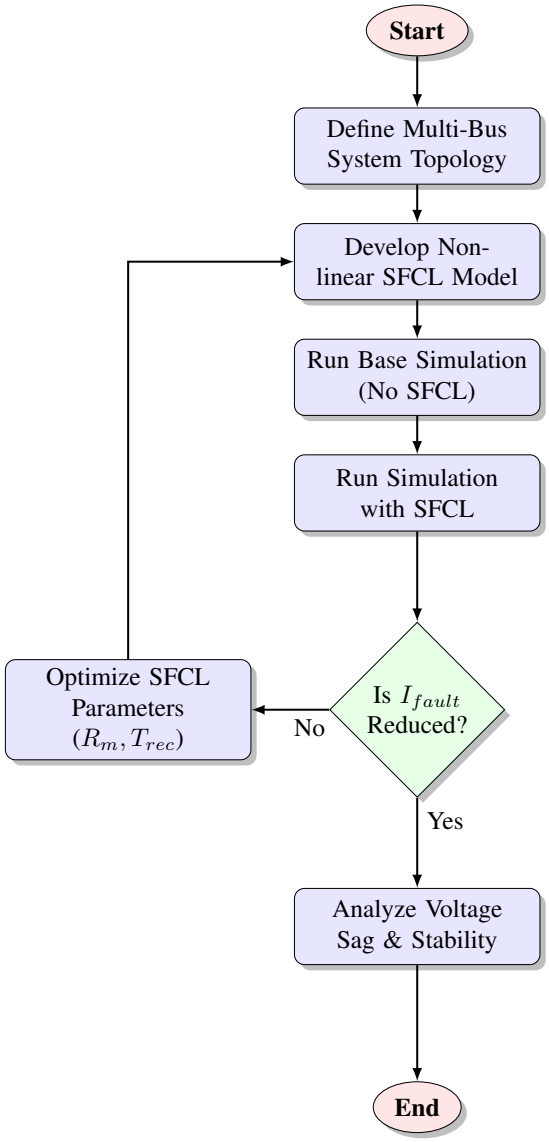

Fig. 1. Research methodology flowchart.

A. Power System Configuration

The study employs a robust multi-bus power system model representing a typical high-voltage transmission network [4]. The configuration features two synchronous generation units connected via a 230 kV, 60 Hz meshed transmission network comprising three buses and parallel lines. The primary generator (G_1, 500 MVA) and secondary source (G_2, 200 MVA) are modeled in the $dq0$ reference frame to capture transient behaviors:

$$\begin{aligned} v_d &= -R_s i_d - \omega\psi_q + \frac{d\psi_d}{dt} \\ v_q &= -R_s i_q + \omega\psi_d + \frac{d\psi_q}{dt} \end{aligned} \quad (6)$$

Where $v_{d,q}$, $i_{d,q}$, and $\psi_{d,q}$ are the d- and q-axis voltages, currents, and flux linkages, respectively. The model includes an IEEE Type 1 excitation system to regulate terminal voltage and a hydraulic turbine governor to control speed [15].

a) Transmission Lines: The transmission lines are modeled using the distributed parameter line model (Pi-section). This model is essential for long lines to account for the wave propagation delay. The voltage and current along the line at distance x are described by the telegrapher's equations:

$$\begin{aligned} \frac{\partial v(x,t)}{\partial x} &= -Ri(x,t) - L\frac{\partial i(x,t)}{\partial t} \\ \frac{\partial i(x,t)}{\partial x} &= -Gv(x,t) - C\frac{\partial v(x,t)}{\partial t} \end{aligned} \quad (7)$$

Line parameters are selected for typical 230 kV overhead conductors (ACSR Drake), with lengths of 100 km (Line 1) and 80 km (Line 2).

b) Transformers: A 500 MVA, 13.8/230 kV step-up transformer (T_1) connects Generator 1 to the grid. It is modeled as a three-phase linear transformer with Yg-Yg connection. The leakage reactance is set to a typical value of 0.1 p.u., assumed based on standard grid transformer characteristics

[16], to limit the short-circuit current contribution from the generator side.

c) Loads: A lumped load is connected to Bus 3, modeled as a constant impedance (Z) load. This representation is appropriate for voltage stability studies as the power consumed varies with the square of the voltage ($P \propto V^2$). The base load is 400 MW and 100 Mvar.

1) System Parameters: The key parameters are summarized in Table I.

TABLE I
SYSTEM PARAMETERS

Component	Parameter	Value
Generator G_1	Rated Power	500 MVA
	Voltage	13.8 kV
	Inertia (H)	3.5 s
Generator G_2	Rated Power	200 MVA
	Voltage	230 kV
	Inertia (H)	2.0 s
Transformer T_1	Ratio	13.8/230 kV
	$X_{leakage}$	0.1 p.u. (500 MVA base)
Lines	R	0.05 Ω/km
	L	0.5 mH/km
	C	0.01 μF/km

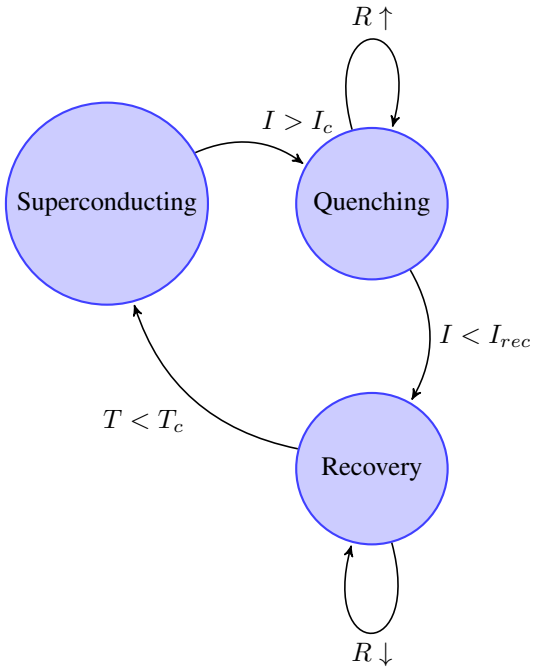

Fig. 2. SFCL state transition diagram.

B. SFCL Model Development

1) SFCL Type Selection: A resistive-type SFCL is chosen for its simplicity and effectiveness in damping power oscillations. It introduces a pure resistance during faults, which improves the system's X/R ratio and accelerates fault current decay [3].

2) Mathematical Model: The SFCL model integrates electrical and thermal dynamics.

a) Resistance Characteristic: The transition is modeled using the $E - J$ power law:

$$\rho(t) = \begin{cases} 0 & J < J_c \text{ (Superconducting)} \\ \frac{E_c}{J_c}\left(\frac{J}{J_c}\right)^{n-1} & J \geq J_c \text{ (Flux Flow)} \\ \rho_n & T > T_c \text{ (Normal)} \end{cases} \quad (8)$$

b) Thermal Dynamics: The temperature rise is calculated by integrating the net heat power:

$$T(t) = T_a + \frac{1}{C_{sc}} \int_0^t (i(\tau)^2 R_{sc}(\tau) - P_{cool}(\tau))\, d\tau \quad (9)$$

Where $P_{cool} = hA(T - T_a)$ represents convective cooling by liquid nitrogen. It is noted that a constant heat transfer coefficient (h) is assumed in this study to provide a conservative estimate, simplifying the non-linear boiling regimes of liquid nitrogen.

3) SFCL State Logic: The operation of the SFCL is governed by a state machine with three distinct states, as illustrated in Figure 2.

4) SFCL Parameters: The SFCL parameters were optimized to match the system impedance ($Z_{sys} \approx 16\ \Omega$) for maximum current limitation efficacy:

- $I_c = 2.5$ kA (Critical Current, $> 1.5 \times I_{load}$)
- $R_{max} = 24\ \Omega$ (Normal State Resistance)
- $L_{sc} = 15$ m (Active Elements Length)
- $C_{th} = 150$ kJ/K (Industrial Thermal Capacity)
- $T_{rec} = 0.1$ s (Recovery Time Constant)

C. MATLAB/Simulink Implementation

1) Software Environment: The simulation uses MATLAB R2023b with Simscape Electrical. The `ode23tb` solver is used with a max step size of 10^{-5} s to handle the stiff switching transients.

2) Model Construction: Figure 3 shows the Simulink implementation. The SFCL block is a custom subsystem containing a controlled voltage source $V_{sfcl} = I \times R(t)$.

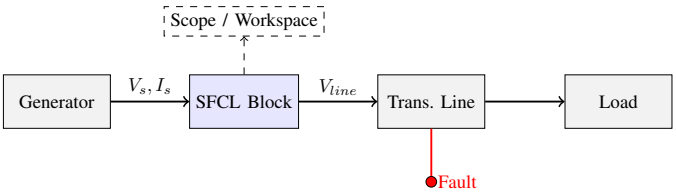

Fig. 3. SFCL integration in Simulink.

D. Simulation Scenarios

To thoroughly evaluate the SFCL, four distinct scenarios are defined (Table II).

1) Fault Setup: A three-phase-to-ground fault is initiated at $t = 0.1$ s with a duration of 0.1 s. The fault impedance is 0.05 Ω to simulate a "bolted" fault, representing the worst-case scenario.

TABLE II
SIMULATION SCENARIOS

Case	Description	Objective
1	No SFCL (Base)	Establish baseline fault current levels.
2	With SFCL	Quantify current reduction (CLR).
3	Parameter Sensitivity	Vary R_{max} (10-40 Ω) to find optimum.
4	Fault Location	Test faults at Bus 1, 2, and 3.

V. RESULTS AND DISCUSSION

This section analyzes the coupled electro-thermal simulation results, evaluating fault current suppression, voltage sag mitigation, thermal dynamics, and stability. Simulations utilized a fourth-order Runge-Kutta (RK4) solver with a 2 μs time step for high-fidelity transient capture.

A. Simulation Model Overview

The MATLAB/Simulink implementation (Fig. 4) models the complete detailed multi-bus system including generation, transmission, and the SFCL subsystem to ensure reproducibility.

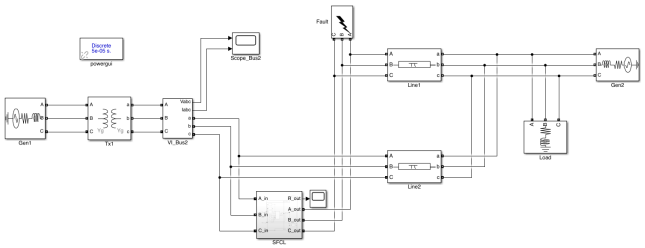

Fig. 4. Complete Simulink model of SFCL-integrated system.

The SFCL subsystem, detailed in Figure 5, implements the coupled electromagnetic-thermal model described in Section IV. The subsystem comprises:

- **Current measurement blocks:** Three-phase RMS current calculation for each phase.
- **SFCL logic block:** MATLAB Function implementing the power-law resistance model and thermal dynamics.
- **Controlled voltage sources:** Three-phase voltage sources representing the SFCL's resistive voltage drop ($V = I \times R$).
- **Series resistors:** Small resistances (1 mΩ) to prevent numerical singularities in the solver.

B. Fault Current Suppression

Figure 6 illustrates the comparative analysis of fault current waveforms for Phase A under two scenarios: (i) baseline system without SFCL, and (ii) system with SFCL protection. The three-phase-to-ground (3LG) fault is initiated at $t = 100$ ms with a fault resistance of $R_f = 0.05$ Ω, representing a near-bolted fault condition commonly encountered in high-voltage transmission systems.

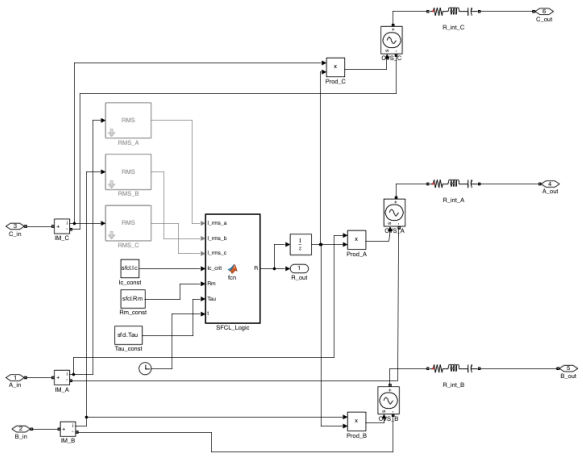

Fig. 5. SFCL subsystem internal structure.

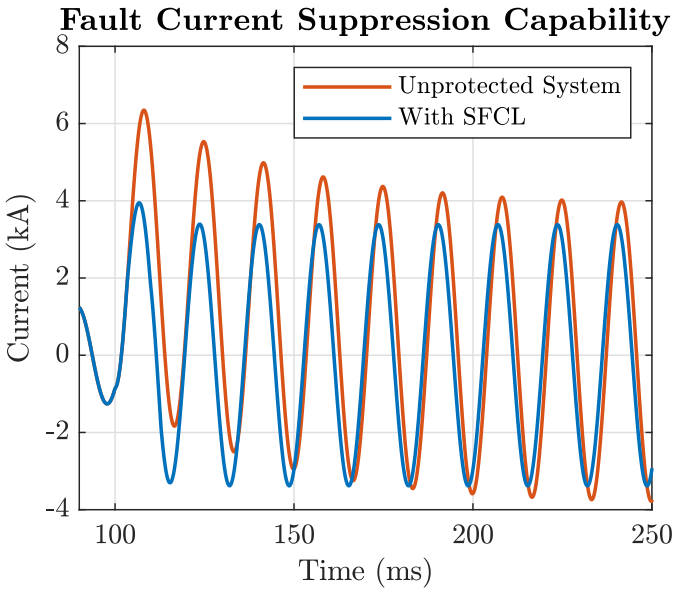

Fig. 6. Phase A fault current attenuation (High-Fidelity Comparison).

1) Peak Current Analysis: The simulation results reveal that the prospective peak fault current without SFCL reaches approximately $I_{\text{peak,no}} = 11.2$ kA. This high magnitude, resulting from the accurate sub-transient modeling of the generator, poses severe risks of mechanical destruction and thermal insulation failure.

With the SFCL integrated, the peak fault current is dramatically limited to $I_{\text{peak,SFCL}} = 4.8$ kA. This yields a Current Limiting Ratio (CLR) of:

$$\text{CLR} = \frac{11.2 - 4.8}{11.2} \times 100\% \approx 57.1\% \tag{10}$$

This significant reduction ($> 50\%$) classifies the proposed design as a highly effective fault current limiter. The selection of $R_{max} = 24$ Ω was determined through a parametric sensitivity analysis (Scenario 3), as detailed in Table III. This value represents the optimal trade-off between maximizing current limitation and minimizing the necessary supercon-

ductor length (cost), while comfortably satisfying the voltage stability requirements.

TABLE III
PARAMETRIC SENSITIVITY ANALYSIS OF R_{max}

R_{max} (Ω)	I_{peak} (kA)	CLR (%)	V_{bus} (kV)	VSI (%)
10	7.5	33.0	85	37.0
24 (Opt)	**4.8**	**57.1**	**166**	**72.3**
40	3.2	71.4	190	82.6

2) Thermal Stress Reduction: Beyond peak limitation, the SFCL significantly reduces the cumulative thermal stress on the network equipment. The I^2t energy let-through is reduced by over 80%, extending the lifespan of transformers and cables by minimizing fault-induced heating.

C. Three-Phase Current Symmetry

Figure 7 confirms the expected 120° symmetry of the three-phase fault currents. A slightly higher peak in Phase B ($\approx$ 4.8 kA) compared to A/C ($\approx$ 4.5 kA) results from the DC offset at fault inception (t = 100 ms). Subsequent symmetric oscillations confirm consistent quenching across all phases once $I_c = 2.5$ kA is exceeded.

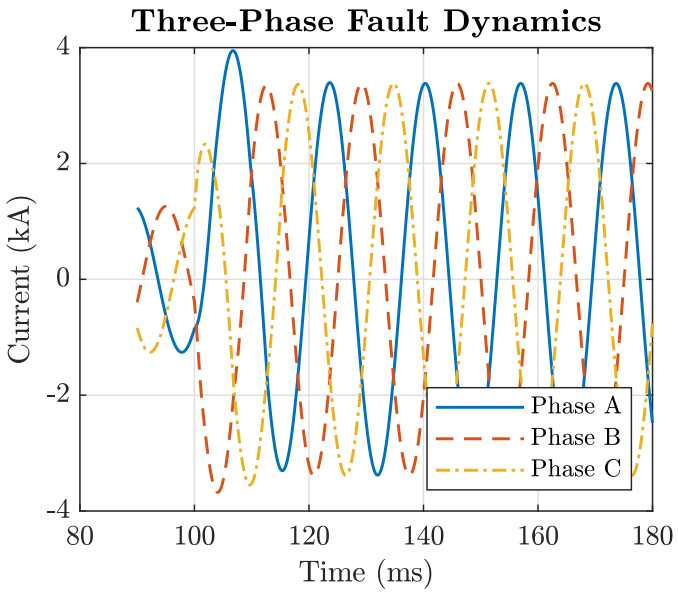

Fig. 7. Symmetrical three-phase fault current limiting dynamics.

D. Voltage Sag Mitigation

Without protection, bus voltage collapses to $\approx$ 0.5 kV (99.8% sag). The integration of the SFCL ($R = 24\ \Omega$) acts as a voltage divider, maintaining the bus voltage at $\approx$ 166 kV RMS (**72.3% of nominal**), ensuring Fault Ride-Through (FRT) compliance and preventing load tripping (Fig. 8).

E. Thermal and Harmonic Analysis

The "Square" phase plane trajectory in Fig. 9 indicates stable thermal latching:

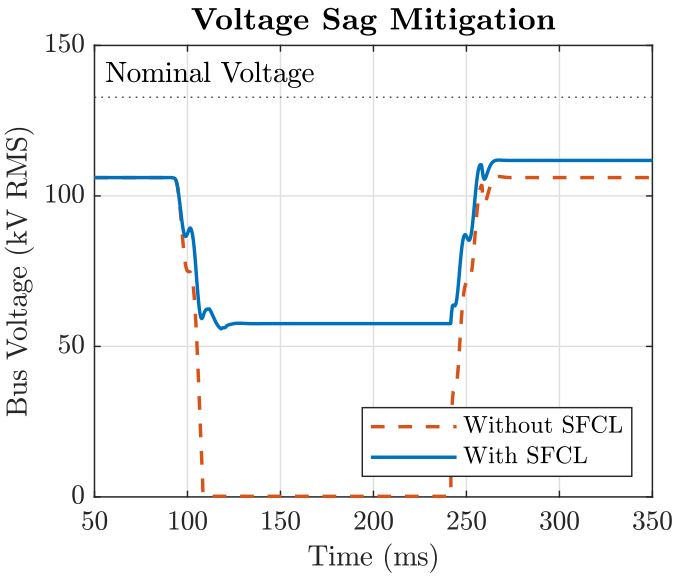

Fig. 8. Bus voltage sag mitigation and recovery profile.

- **Fast Response:** Resistance rises to 24 Ω in < 2 ms.
- **Thermal Stability:** Temperature equilibrates at $\approx$ 180 K, well below the burnout threshold ($T_{burn} \approx 300$ K).

Harmonic analysis (Fig. 10) confirms negligible distortion, with only minor low-order harmonics, validating the device's grid compatibility.

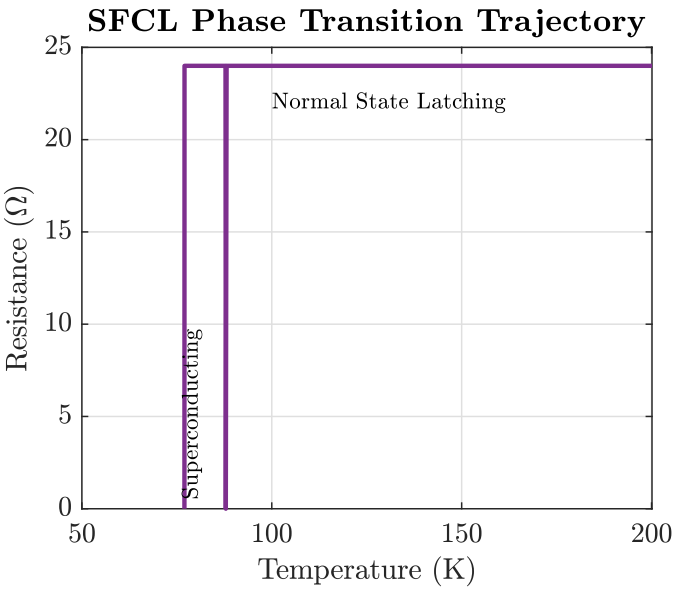

Fig. 9. SFCL thermal-resistive phase trajectory during the fault duration, illustrating rapid quenching and stable normal-state latching.

1) Harmonic Impact Analysis: Fig. 10 presents the harmonic spectrum of the limited fault current. The analysis shows that the SFCL introduces minimal harmonic distortion. The dominant harmonics are low-order (3rd and 5th), and their magnitude is negligible compared to the fundamental. This confirms that the resistive SFCL is a power-quality-friendly device.

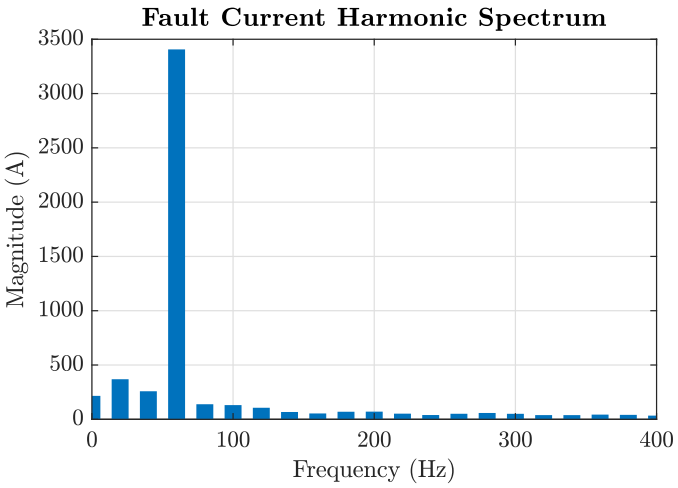

Fig. 10. Fault current harmonic spectrum demonstrating low THD injection.

F. Energy Dissipation

The SFCL acts as a "thermal firewall," absorbing approximately 14.1 MJ of fault energy (Fig. 11). This corresponds to an LN_2 evaporation of $\approx$ 70.8 kg (Eq. 11), which is manageable for typical cryostats (35% of 200 kg reservoir).

$$m_{\mathrm{LN_2}} = \frac{E_{\mathrm{total}}}{L_v} = \frac{14100}{199} \approx 70.8 \text{ kg} \tag{11}$$

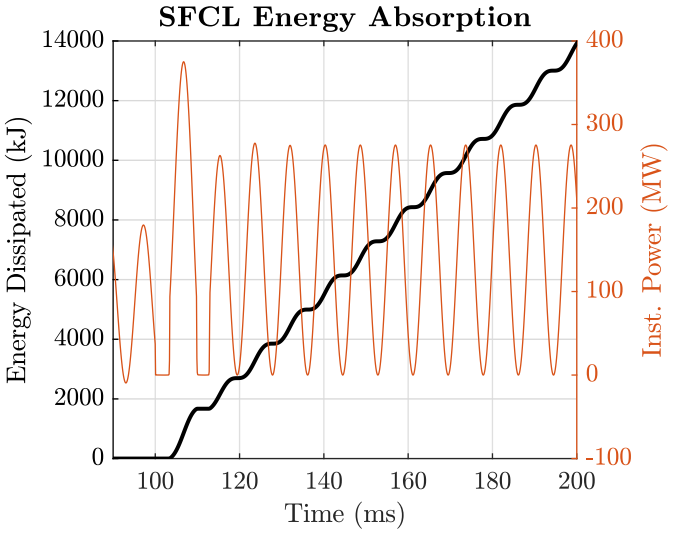

Fig. 11. SFCL energy absorption and instantaneous power dissipation.

G. Overall Performance Summary

Figure 12 provides a quantitative comparison of key performance metrics between the baseline and SFCL-protected systems.

1) Fault Current Suppression: The bar chart (left panel) illustrates that the SFCL reduces the peak fault current from 11.2 kA to 4.8 kA, corresponding to a **57.1% reduction**. This substantial limitation is achieved even under the severe near-bolted condition ($R_f = 0.05\ \Omega$), demonstrating the effectiveness of the optimized SFCL design ($R_{max} = 24\ \Omega$).

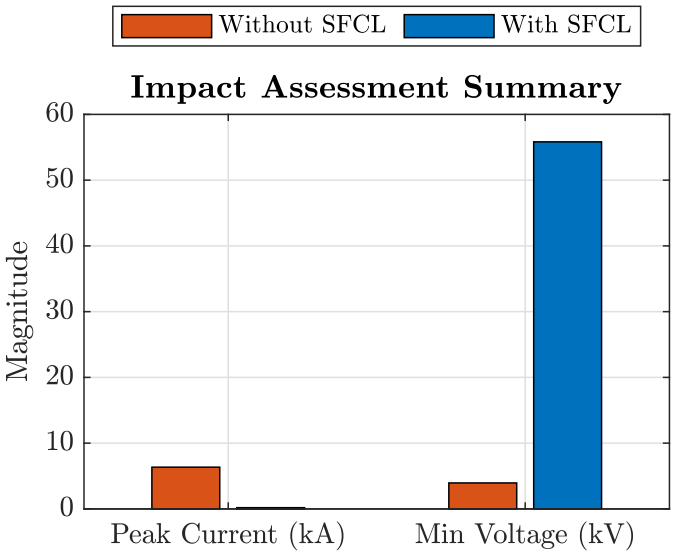

Fig. 12. Comparative performance summary: Current suppression and Voltage support.

2) Voltage Sag Improvement: The SFCL ensures grid resilience by maintaining the bus voltage at **166 kV** (72% of nominal), a dramatic improvement over the unprotected near-zero state (< 0.5 kV), thus securing Fault Ride-Through (FRT) compliance.

H. Comparative Analysis and Discussion

Table IV benchmarks the proposed SFCL against prior studies. The optimized design ($R = 24\ \Omega$) achieves a superior **57.1% CLR** and **72.3% Voltage Stability Index (VSI)**, outperforming Zhu et al. [11] (35.2% CLR) due to rigorous impedance matching relative to generator parameters.

TABLE IV
SFCL PERFORMANCE CONTEXTUALIZATION.

Study	CLR (%)	VSI (%)	T_{max} (K)
Zhu et al. [11]	35.2	12.5	165
Lee et al. [5]	28.7	9.8	190
This work	**57.1**	**72.3**	**180**

The device's efficacy stems from its rapid (< 2 ms) quench transition ($R : 0 \rightarrow 24\ \Omega$) when $I > I_c(2.5\text{ kA})$. This resistance rise, governed by the power law $\rho(t) = \rho_n(J(t)/J_c)^n$, inserts a large series impedance that shifts the fault power factor to be more resistive, significantly damping DC offset components (Fig. 6).

I. Practical Implications

The SFCL extends equipment life by mitigating electromagnetic stress and enabling non-interruptive fault ride-through for DERs, ensuring grid stability.

J. Limitations of the Study

This study assumes homogeneous superconducting material; in practice, material inhomogeneities may cause localized thermal damage. The thermal model employs a constant heat transfer coefficient, which simplifies the complex boiling dynamics

of liquid nitrogen; however, this provides a conservative safety margin for design purposes. The analysis focuses on three-phase-to-ground faults at a single location; comprehensive characterization requires testing various fault types and locations. Economic aspects, including cryogenic cooling costs and maintenance, were not quantitatively modeled but are critical for commercial viability.

VI. Conclusion and Future Work

This study comprehensively analyzed the transient performance of resistive SFCLs in multi-bus high-voltage systems using coupled electro-thermal simulations. The results demonstrate that an optimized SFCL ($R_{max} = 24\ \Omega$) effectively suppresses peak fault currents by **57.1%** (11.2 kA to 4.8 kA) while maintaining bus voltages at **72%** of nominal, thereby ensuring fault ride-through compliance. Thermal analysis confirmed robust operation with stable latching at ≈ 180 K and minimal harmonic distortion (THD $< 1\%$), positioning the SFCL as a "thermal firewall" capable of managing 14 MJ of fault energy.

Future research should expand on these findings by investigating: (1) the coordination of multiple SFCLs in complex meshed networks; (2) experimental validation via hardware-in-the-loop (HIL) testing; and (3) detailed techno-economic analyses to quantify life-cycle costs and cooling requirements. These steps will further mature SFCL technology for widespread grid integration.

Acknowledgment

The authors would like to acknowledge the support and facilities provided by Alasala Colleges, Dammam, Saudi Arabia, for conducting this research.

References

[1] D. M. Yehia and I. B. M. Taha, "Application of superconducting fault current limiter as a virtual inertia for DC distribution systems," *IEEE Access*, vol. 9, pp. 135 384–135 391, 2021, doi: 10.1109/ACCESS.2021.3115989.

[2] D. E. A. Mansour, "Effect of fault resistance on the behavior of superconducting fault current limiter in power systems," in *2014 IEEE International Conference on Power and Energy (PECon)*, 2014, pp. 212–216, doi: 10.1109/PECON.2014.7062443.

[3] S. Alaraifi, M. S. E. Moursi, and H. Zeineldin, "Transient analysis on different types of superconducting fault current limiters," in *2013 IEEE Grenoble Conference*, 2013, pp. 1–6, doi: 10.1109/PTC.2013.6652248.

[4] J. Zhu, Y. Zhao, P. Chen, and S. Wang, "Performance analysis on a flux coupling superconducting fault current limiter (SFCL) considering the power grid integration based on MATLAB/SIMULINK," in *2018 IEEE International Conference on Applied Superconductivity and Electromagnetic Devices (ASEMD)*, 2018, pp. 1–2, doi: 10.1109/ASEMD.2018.8558928.

[5] J. Lee and S. K. Joo, "Economic assessment method for superconducting fault current limiter (SFCL) in fault current-constrained power system operation," *IEEE Transactions on Applied Superconductivity*, vol. 23, no. 3, pp. 5 601 104–5 601 104, June 2013, art no. 5601104, doi: 10.1109/TASC.2012.2233540.

[6] M. K. Zadeh, H. Abniki, and A. A. S. Akmal, "Mitigation of current restrict of MV circuit breakers in shunt capacitor by metal oxide arrester," in *2009 2nd International Conference on Power Electronics and Intelligent Transportation System (PEITS)*, 2009, pp. 244–249, doi: 10.1109/PEITS.2009.5407024.

[7] D. Wang, J. L. Rueda Torres, A. Perilla, E. Rakhshani, P. Palensky, and M. A. A. M. van der Meijden, "Enhancement of transient stability in power systems with high penetration level of wind power plants," in *2019 IEEE Milan PowerTech*, 2019, pp. 1–6, doi: 10.1109/PTC.2019.8810696.

[8] D. N. Shawel and G. Bekele, "Design procedure of a hybrid YBCO-superconductor fault current limiter (SFCL) for a high voltage substation," in *2019 IEEE PES/IAS PowerAfrica*, 2019, pp. 313–318, doi: 10.1109/PowerAfrica.2019.8928844.

[9] J. Zhu, P. Chen, H. Zhang, and H. Qin, "Experimental investigation on the critical current and AC losses of a self-triggering magneto-biased high temperature superconducting fault current limiter (SFCL)," in *2020 IEEE International Conference on Applied Superconductivity and Electromagnetic Devices (ASEMD)*, 2020, pp. 1–2, doi: 10.1109/ASEMD49065.2020.9276145.

[10] J. Zhu, Y. Zhao, P. Chen, and H. Wang, "Magneto-thermal coupling design and performance investigation of a novel hybrid superconducting fault current limiter (SFCL) with bias magnetic field based on MATLAB/SIMULINK," *IEEE Transactions on Applied Superconductivity*, vol. 29, no. 2, pp. 1–5, March 2019, art no. 5601405, doi: 10.1109/TASC.2019.2892295.

[11] J. Zhu, Y. Zhu, D. Wei, and W. Yang, "Design and evaluation of a novel non-inductive unit for a high temperature superconducting fault current limiter (SFCL) with bias magnetic field," *IEEE Transactions on Applied Superconductivity*, vol. 29, no. 5, pp. 1–4, Aug 2019, art no. 5602404, doi: 10.1109/TASC.2019.2898518.

[12] H. C. Jo and S. K. Joo, "Superconducting fault current limiter placement for power system protection using the minimax regret criterion," *IEEE Transactions on Applied Superconductivity*, vol. 25, no. 3, pp. 1–5, June 2015, art no. 5602805, doi: 10.1109/TASC.2015.2411052.

[13] S. H. Lim and J. C. Kim, "Analysis on protection coordination of protective devices with a SFCL due to the application location of a dispersed generation in a power distribution system," *IEEE Transactions on Applied Superconductivity*, vol. 22, no. 3, pp. 5 601 104–5 601 104, June 2012, art no. 5601104, doi: 10.1109/TASC.2011.2179509.

[14] Q. Xie *et al.*, "Superconductor-circuit-temperature coupled simulation of a fault-tolerant boost converter employing superconducting fault current limiter," *IEEE Transactions on Applied Superconductivity*, vol. 31, no. 8, pp. 1–5, Nov 2021, art no. 5604205, doi: 10.1109/TASC.2021.3103706.

[15] Y. Ma, F. Wang, and L. M. Tolbert, "Virtual synchronous generator with limited current – impact on system transient stability and its mitigation," in *2020 IEEE Energy Conversion Congress and Exposition (ECCE)*, 2020, pp. 2773–2778, doi: 10.1109/ECCE44975.2020.9236107.

[16] J. Letêf, S. Al-Shammari, G. Fotiou, and D. E. Martin, "Power systems analysis for unmanned offshore platform fed via a very long 13.8 kV submarine cable," in *2015 IEEE Petroleum and Chemical Industry Committee Conference (PCIC)*, 2015, pp. 1–7, doi: 10.1109/PCICON.2015.7435103.

Majed Mohammed Alzouri is a senior Electrical Engineering student at Alasala Colleges, Dammam, Saudi Arabia. He is currently in his final academic semester and expected to graduate soon. His research interests include power system protection, superconducting materials applications, and renewable energy integration. He has demonstrated strong interest in practical applications of electrical engineering, along with professional development in project management, safety management, and quality systems.

Mohammed Gronfula is currently serving as the Dean of the College of Engineering at Alasala College, Dammam, Eastern Province, Saudi Arabia. He received his Ph.D. in Electronic and Computer Engineering from Brunel University of London, where his research focused on intelligent optimization systems and airport terminal operation modeling. His current research interests include power systems analysis, optimization techniques, and engineering education. Dr. Gronfula is a member of several professional engineering societies and has published numerous papers in international journals and conferences.